Letter

First measurement of ΛN inelastic scattering with Λ from $e^+e^- \rightarrow J/\psi \rightarrow \Lambda\bar{\Lambda}$

M. Ablikim *et al.**
(BESIII Collaboration)

(Received 10 October 2023; accepted 12 April 2024; published 14 May 2024)

Using an e^+e^- collision data sample of $(10\,087 \pm 44) \times 10^6$ J/ψ events taken at the center-of-mass energy of 3.097 GeV by the BESIII detector at the BEPCII collider, the process $\Lambda + N \rightarrow \Sigma^+ + X$ is studied for the first time employing a novel method. The Σ^+ hyperons are produced by the collisions of Λ hyperons from J/ψ decays with nuclei in the material of the BESIII detector. The total cross section of $\Lambda + {}^9\mathrm{Be} \rightarrow \Sigma^+ + X$ is measured to be $\sigma = (37.3 \pm 4.7 \pm 3.5)$ mb with Λ momenta within [1.057, 1.091] GeV/c, where the uncertainties are statistical and systematic, respectively. This analysis is the first study of Λ-nucleon interactions at an e^+e^- collider, providing information and constraints relevant for the strong-interaction potential, the origin of color confinement, the unified model for baryon-baryon interactions, and the internal structure of neutron stars.

DOI: 10.1103/PhysRevC.109.L052201

Describing baryon-baryon interactions within a unified model has always been a challenge in both particle and nuclear physics [1–4]. Strong constraints and well-established models exist for nucleon-nucleon interactions [1,2], but there are still difficulties in precisely modeling hyperon-nucleon scattering, especially hyperon-hyperon interactions, due to the lack of experimental measurements. Until now, there have only been a few measurements for hyperon-nucleon scattering [5–17], and only one for hyperon-hyperon scattering [18], leaving theoretical models largely unconstrained [19–34].

The properties of hyperons in dense matter have attracted much interest due to their close connection with hypernuclei and the hyperon component in neutron stars [4]. Hyperons may exist within the inner layer of neutron stars whose structure strongly depends on the equation of state (EOS) of nuclear matter at supersaturation densities [35]. The appearance of hyperons in the core softens the EOS, resulting in neutron stars with masses lower than $2M_\odot$ [36], where $M_\odot$ is the mass of the sun. However, studies based on observations from the LIGO and Virgo experiments [37] indicate that the EOS can support neutron stars with masses above $1.97M_\odot$. This is the so-called "hyperon puzzle in neutron stars," warranting further experimental and theoretical studies.

The first attempts to measure hyperon-nucleon interactions ($\Lambda p \rightarrow \Lambda p$, $\Sigma^- p \rightarrow \Sigma^- p/\Lambda n/\Sigma^0 n$, and $\Sigma^+ p \rightarrow \Sigma^+ p$) were made during the 1960s and 1970s using hyperons with momenta less than 1 GeV/c [5–9]. After a gap of about 20 years, further studies of elastic and inelastic scatterings between hyperons and nucleons were performed using multiple kinds of hyperons with a variety of beam energies [10–17]. The uncertainties on these measurements were, in general, large. On the theoretical side, many models have been proposed to describe the hyperon-nucleon and hyperon-hyperon interactions, including the meson-exchange model (with Jülich [19] or Nijmegen [20] potentials), chiral effective field theory (χEFT) approaches [21–28], calculations on the lattice from HALQCD [29,30] and NPLQCD [31,32], low-momentum models [33], and quark-model approaches [34].

Experimental studies of hyperon-nucleon interactions are challenged by the difficulty of obtaining a stable hyperon beam. Firstly, the lifetime of ground-state hyperons is usually of order $O(10^{-10})$ s due to the weak decay, which is too short to provide a stable beam. Meanwhile, hyperons historically used for fixed-target experiments are commonly produced in the collisions between incident protons or K mesons and the target material, with a high background level. Compared with fixed-target experiments, many more hyperons are accessible from the decay of charmonia produced at e^+e^- colliders, which have rarely been used to study hyperon-nucleon scattering because of the lack of both specialized targets and any practical experimental approach. Furthermore, the large number of antihyperons produced in pairs with hyperons bring exciting prospects for probing little-studied antihyperon-nucleon interactions. In this work, the $\Lambda + N \rightarrow \Sigma^+ + X$ process is studied for the first time by a novel method [38,39], where N denotes a certain kind of nucleus and X refers to any possible particles produced accompanying the Σ^+, using $\Lambda\bar{\Lambda}$ pairs from the decay of $(10087 \pm 44) \times 10^6$ J/ψ events collected by BESIII [40,41]. This method has been applied in a recent BESIII study of Ξ^0-nucleus interaction [17]. Thanks to the 'double-tag" method, a nearly monochromatic hyperon flux of Λ, Σ^+, Σ^-, Ξ^-, Ξ^0, Ω^-, and their antiparticles from charmonia decay are accessible that allows for the study of hyperon-nucleon interactions at e^+e^- colliders.

The BESIII detector is a magnetic spectrometer [42] located at the Beijing Electron Positron Collider (BEPCII). The cylindrical core of the BESIII detector consists of a helium-based multilayer drift chamber (MDC), a plastic scintillator time-of-flight (TOF) system, and a CsI(Tl) electromagnetic calorimeter (EMC), which are all enclosed in a superconducting solenoidal magnet providing a 1.0-T magnetic field. Before particles produced in e^+e^- collisions enter the

*Full author list given at the end of the article.

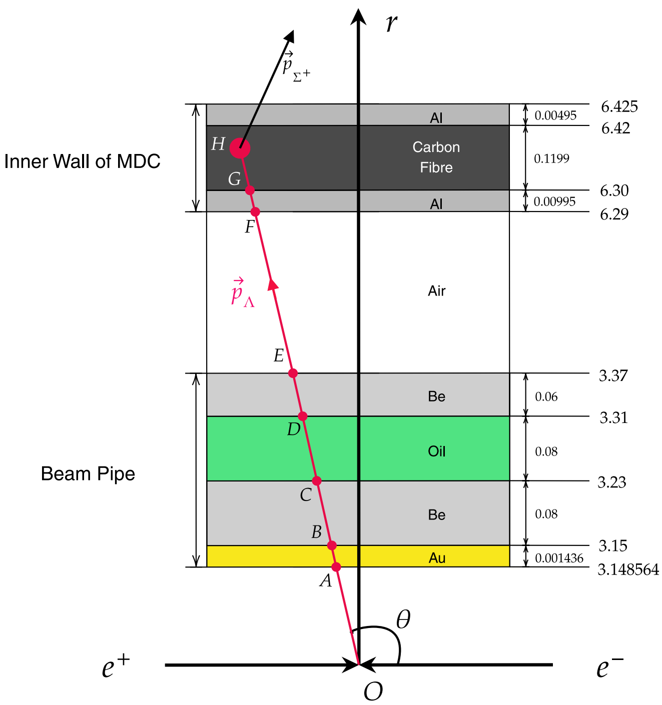

FIG. 1. Illustration of target structure and Λ trajectory inside the target. The target material, composed of the beam pipe and inner wall of the MDC, consists of multiple layers of material, including gold, beryllium, oil, aluminum, and carbon fiber. O is the interaction point of the e^+e^- collision. The horizontal axis is the e^+e^- beam line and the vertical axis (r axis) denotes the distance away from the beam line. The radius and the length of the inner wall of the beam pipe from and along the z axis are 3.148 564 and 100 cm, respectively [42]. The position and the thickness of each layer are listed in the figure, where the units are centimeters. θ is the angle between incident Λ and the z axis. H is the scattering point of Λ and nucleon so that $AB, BC, \ldots, GH$ are the Λ track lengths in each layer, where the sum is the total track length inside the target.

spectrometer, they pass through the beam pipe and the inner wall of the MDC, which constitute the scattering targets in the present study. The target structure and the Λ trajectory are shown in Fig. 1, where the Λ hyperons can scatter elastically or inelastically with the nuclei inside these objects. The target is made of multiple layers with different materials, with more detailed information given in Sect. I of the Supplemental Material [43].

Using a GEANT4-based [44] Monte Carlo (MC) package, simulated samples are produced incorporating the geometric description [45] of the BESIII detector and the detector response. An inclusive MC sample containing 1×10^{10} J/ψ decays is used to investigate the potential backgrounds. The production of the J/ψ resonance is simulated by the MC event generator KKMC [46], where the beam-energy spread and the initial-state radiation in the e^+e^- annihilation have been taken into account. The known decay modes are generated by EVTGEN [47,48] using branching fractions taken from the Particle Data Group (PDG) [49], while the unknown decay modes are modeled with LUNDCHARM [50,51]. A signal MC sample with 1×10^6 $\Lambda N \to \Sigma^+ X$, $\Sigma^+ \to p\pi^0$ events is generated to estimate the detection efficiency. The angular distributions of $J/\psi \to \Lambda\bar{\Lambda}$ and $\bar{\Lambda} \to \bar{p}\pi^+$ are described by the recently measured decay parameters of the J/ψ and Λ hyperons [52] and $\Lambda N \to \Sigma^+ X$, $\Sigma^+ \to p\pi^0$ processes are simulated by the Bertini intranuclear cascade model [53] of the QGSP_BERT physics list defined in GEANT4 [44].

Since Λ and $\bar{\Lambda}$ are produced in pairs from $J/\psi \to \Lambda\bar{\Lambda}$ decays, the detection of a single $\bar{\Lambda}$ hyperon in an event (called "single-tag") implies that the recoiling system is a monochromatic Λ hyperon. In this analysis, the $\bar{\Lambda}$ hyperon is reconstructed via $\bar{\Lambda} \to \bar{p}\pi^+$ and the yield of single-tagged events is obtained by fitting to the recoil-mass distribution of the $\bar{\Lambda}$ hyperon, denoted as $N_{\rm ST}$. The recoil mass of the $\bar{\Lambda}$ hyperson is defined as $RM_{\bar{p}\pi^+} = \sqrt{|p_{e^+e^-} - p_{\bar{p}} - p_{\pi^+}|^2}$, where $p_{e^+e^-}$, $p_{\bar{p}}$ and p_{π^+} refer to the four-momenta of the initial e^+e^-, $\bar{p}$, and π^+ particles, respectively. The recoiling Λ hyperon produced together with the reconstructed $\bar{\Lambda}$ hyperon can scatter inelastically with the nucleons in the material and produce a Σ^+ hyperon. We search for such particles through the decay $\Sigma^+ \to p\pi^0$ among the other tracks and showers in the event, excluding those used to reconstruct the single-tagged $\bar{\Lambda}$ hyperon. The number of double-tagged events ($N_{\rm DT}$) containing both a reconstructed $\bar{\Lambda}$ hyperon and a Σ^+ hyperon is given by

$$N_{\rm DT} = \mathcal{L}_\Lambda \cdot \sigma(\Lambda N \to \Sigma^+ X) \cdot \mathcal{B}(\Sigma^+ \to p\pi^0) \cdot \epsilon_{\rm sig}, \quad (1)$$

where $\sigma(\Lambda N \to \Sigma^+ X)$ is the cross section of the inelastic process $\Lambda N \to \Sigma^+ X$, $\mathcal{B}(\Sigma^+ \to p\pi^0)$ is the branching fraction of $\Sigma^+ \to p\pi^0$ decay, and $\epsilon_{\rm sig}$ denotes the efficiency of the double-tag reconstruction. The "effective luminosity" $\mathcal{L}_\Lambda$ is a specially defined quantity to describe the property of the target and the behavior of the incident Λ particle inside the target, which is influenced by several other parameters [15]. Considering the target composition shown in Fig. 1, $\mathcal{L}_\Lambda$ is calculated event by event as

$$\mathcal{L}_\Lambda = N_{\rm ST} \frac{N_A}{N_{\rm ST}^{\rm MC}} \sum_j^7 \sum_i^{N_{\rm ST}^{\rm MC}} \frac{\rho_T^j l^{ij}}{M^j} \mathcal{R}_\sigma^j, \quad (2)$$

where N_A is Avogadro's number [54], $N_{\rm ST}^{\rm MC}$ is the total number of single-tagged events in the signal MC sample, l^{ij} is the path length of the incident Λ particle of the $i_{\rm th}$ event inside the $j_{\rm th}$ layer, and M^j and ρ_T^j are the molar mass [55] and density, respectively, of the $j_{\rm th}$ layer. Since the contribution from each layer and the cross section for different kinds of nuclei are not the same, the ratio of the scattering cross section ($\mathcal{R}_\sigma$) of incident Λ for each category of materials is necessary for normalization. In this Letter, we present the measured cross section of the $\Lambda + {}^9\text{Be} \to \Sigma^+ + X$ reaction, with the cross section of each material normalized to that of beryllium. The choice of beryllium as the normalization reference is due to its common use as the target in fixed-target experiments and its significance as the main material of the beam pipe in the BESIII detector. In the case of low and intermediate energy it is assumed that inelastic scattering occurs with single protons on the surface of the nucleus [56–61]. Then $\mathcal{R}_\sigma$ is proportional to $A^{\frac{2}{3}} \times \frac{Z}{A} = \frac{Z}{A^{\frac{1}{3}}}$, where A and Z are the numbers of nucleons and protons in a single nucleus, respectively. If the material of a certain layer contains multiple kinds of nuclei, $\mathcal{R}_\sigma$ must be weighted by the ratio of the numbers of different nuclei per unit volume of the material. The detailed derivation and calculation of $\mathcal{L}_\Lambda$ can be found in Sec. II of the Supplemental Material [43].

According to Eq. (1), the cross section for interaction with the Be nucleus can be determined as

$$\sigma(\mathrm{Be}) = \frac{N_{\mathrm{DT}}}{\epsilon_{\mathrm{sig}}\mathcal{L}_\Lambda}\frac{1}{\mathcal{B}(\Sigma^+ \to p\pi^0)}. \tag{3}$$

Since we only reconstruct the Σ^+ on the double-tag side, there may also be contributions from the interactions between the Λ and neutrons. However, the contributions can only arise from three-body reactions such as $\Lambda n \to \Sigma^+ n\pi^-$. The total energy in the center-of-mass frame of Λ and a stationary neutron is [2.240, 2.249] GeV, while the lowest total energy for the final state $\Sigma^+ n\pi^-$ is 2.269 GeV. Therefore, this process can only occur when the neutrons have relatively large Fermi momenta. As a result, the cross section is suppressed due to the limited phase space. Similar reactions such as $\Lambda p \to \Sigma^- p\pi^+/\Sigma^+ p\pi^-$ have been studied [9], which for Λ momentum within [1.057, 1.091] GeV/c are at least 1 order of magnitude smaller than the measured cross section of $\Lambda p \to \Sigma^+ X$. Therefore, we neglect the contribution from Λn reactions.

We now describe the selection of signal events. Charged tracks detected in the MDC are required to have a polar angle (θ) satisfying $|\cos\theta| < 0.93$ with respect to the positron beam. The number of good charged tracks must be at least two.

For the single-tag side, $\bar{\Lambda}$ is reconstructed from its decay to $\bar{p}$ and π^+, which are identified using the measured information in the MDC and TOF. The combined likelihoods ($\mathcal{L}$) under the proton (antiproton), pion, and kaon hypotheses are calculated. The $\bar{p}$ candidates are required to satisfy $\mathcal{L}(p) > \mathcal{L}(K)$ and $\mathcal{L}(p) > \mathcal{L}(\pi)$, whereas the π^+ candidates are required to satisfy $\mathcal{L}(\pi) > \mathcal{L}(K)$. A vertex fit is performed to constrain all possible $\bar{p}\pi^+$ combinations to a common vertex. The decay length of $\bar{\Lambda}$ is calculated as the distance between the fitted vertex and the interaction point (IP) of the e^+e^- collision. The $\bar{p}\pi^+$ combinations with a vertex-fit χ^2 lower than 200 and a decay length larger than 0 are regarded as $\bar{\Lambda}$ candidates. To further suppress the background, the invariant masses of the $\bar{p}\pi^+$ combinations are required to lie within [1.111, 1.120] GeV/c^2 and $RM_{\bar{p}\pi^+}$ is required to be within [1.071, 1.153] GeV/c^2. If there are multiple candidates passing all the selection criteria above, we select the $\bar{p}\pi^+$ combination with the minimum vertex-fit χ^2 as the best candidate. The number of single-tagged events is determined to be $7\,207\,565 \pm 3741$ by fitting to the $RM_{\bar{p}\pi^+}$ distribution using the sum of two Gaussian distributions and a second-order Chebyshev polynomial, as shown in Fig. 2. The efficiency of the single-tag selection is $(52.16 \pm 0.10)\%$.

In the double-tag selection Σ^+ candidates are reconstructed in the $p\pi^0$ final state. The p is selected using the same criteria as the single-tag selection and the π^0 is reconstructed through EMC showers. The deposited energy of each shower must be more than 25 MeV in the barrel region ($|\cos\theta| < 0.80$) and more than 50 MeV in the end-cap region ($|\cos\theta| < 0.92$) of the EMC. To suppress electronic noise and showers unrelated to the event, the difference between the EMC time and the event-start time is required to be within [0, 700] ns. The angle between photons and all the other charged tracks should be larger than 10° to suppress the photons from the radiation of charged tracks and other processes. Then a kinematic fit is performed to all possible combinations of two showers by constraining the invariant mass $M_{\gamma\gamma}$ to the known π^0 mass [49]. The combination with the minimum χ^2 from this fit is chosen as the π^0 candidate. The Σ^+ candidate is selected from $p\pi^0$ combinations with invariant mass $M_{p\pi^0} \in [1.12, 1.25]$ GeV/c^2 that has the maximum value of $\mathcal{L}(p)$ for the proton candidate.

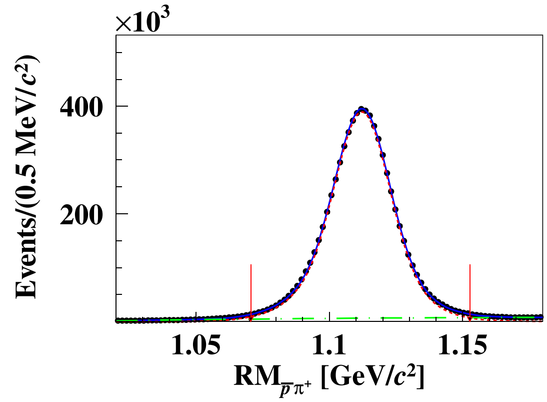

FIG. 2. The $RM_{\bar{p}\pi^+}$ distribution with the fit result superimposed. The black dots with error bars represent the data. The blue solid line is the total fit. The dashed red line is the signal of the single-tag selection and the dot-dashed green line is the background. The red arrows indicate the signal range.

If the incident Λ does not scatter with any nucleons, the recoil mass of $\bar{p}\pi^+p$, $RM_{\bar{p}\pi^+p}$, should be around the known mass of π^- [49] according to the kinematic constraint. For inelastic scattering events, $RM_{\bar{p}\pi^+p}$ has a tendency to be negative, as seen with the signal MC sample and discussed in Sec. III of the Supplemental Material [43]. This behavior is explained by the additional mass and momentum contributed by nucleons in the reaction. To further suppress the background, $RM_{\bar{p}\pi^+p}$ is required to be negative. In addition, the normal event of $J/\psi \to \Lambda\bar{\Lambda}$ without the hyperon-nucleus scattering can be rejected by identifying a Λ hyperon in the double-tag side after the Σ^+ candidate reconstruction using all possible $p\pi^-$ combinations. The Λ candidate is rejected if $M_{p\pi^-} \in [1.108, 1.124]$ GeV/c^2.

The number of double-tagged events is found to be 795 ± 101 by fitting to the distribution of $M_{p\pi^0}$ using a sum of two Gaussian distributions and a third-order Chebyshev polynomial, as is shown in Fig. 3. The parameters and fraction of the two Gaussian distributions are fixed to those obtained from the same fit to the signal MC sample. The efficiency of the double-tag selection is estimated to be $\epsilon_{\mathrm{sig}} = (24.32 \pm 0.15)\%$ by fitting the signal MC sample.

The cross section of $\Lambda + {}^9\mathrm{Be} \to \Sigma^+ + X$ is determined through Eq. (3) to be $\sigma(\Lambda + {}^9\mathrm{Be} \to \Sigma^+ + X) = (37.3 \pm$

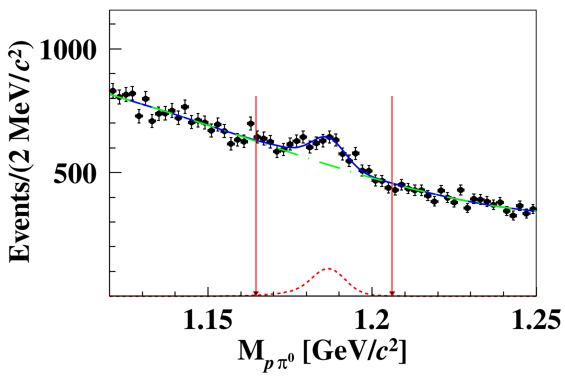

FIG. 3. The $M_{p\pi^0}$ distribution with the fit result overlaid. The black dots with error bars represent the data. The blue solid line is the total fit. The dashed red line is the signal and the dot-dashed green line is the background. The red arrows indicate the signal range.

$4.7_{\mathrm{stat.}} \pm 3.5_{\mathrm{syst.}}$) mb, where $\mathcal{B}(\Sigma^+ \to p\pi^0)$ is taken from the PDG [49]. Table I lists the inputs used in the calculation.

The systematic uncertainty for the measured cross section is associated with the knowledge of the tracking and particle identification (PID) efficiencies of charged particles, the reconstruction efficiency of π^0 mesons, the number of single-tagged events, the efficiency of the requirement of $RM_{\bar{p}\pi^+p}$ and $M_{p\pi^-}$,the angular distribution of $J/\psi \to \Lambda\bar{\Lambda}$ and Σ^+, the size of the signal MC sample, the measured interaction point of the e^+e^- collision, the method to fit the $M_{p\pi^0}$ distribution, and the luminosity ($\mathcal{L}_\Lambda$) estimation. The assumption concerning the ratio of cross sections for different kinds of nuclei also introduces a systematic uncertainty.

The systematic uncertainties related to the tracking and PID efficiencies of protons are both 1.0% [62], and for π^0 reconstruction the systematic uncertainty is 1.0% [63]. The systematic uncertainty associated with the number of the single-tagged events is determined to be 0.8% from the inclusive MC. The systematic uncertainties from the $RM_{\bar{p}\pi^+p}$ and $M_{p\pi^-}$ requirements are tested by varying the criteria around the baseline settings to reobtain the measured cross section. The changes of the cross section are denoted as $\Delta = |\sigma - \sigma_{\mathrm{sys.}}|$, where σ and $\sigma_{\mathrm{sys.}}$ refer to the baseline results and the results after changing the criteria. Also calculated are the uncorrelated uncertainties $\omega_{\mathrm{uc.}} = \sqrt{|\omega_\sigma^2 - \omega_{\sigma,\mathrm{sys.}}^2|}$, where ω_σ and $\omega_{\sigma,\mathrm{sys.}}$ correspond to the fit uncertainties of the baseline and systematic test results, respectively. Since the ratio $\Delta/\omega_{\mathrm{uc.}}$ does not show a trending behavior and is less than 2, these two possible sources of systematic bias are considered to be negligible [64]. The systematic uncertainty associated with the knowledge of the angular distribution of $J/\psi \to \Lambda\bar{\Lambda}$ production is estimated by varying the decay parameters $\alpha_{J/\psi}$, $\Delta\Phi$, α_Λ, and $\alpha_{\bar{\Lambda}}$ within 1 standard deviation [52] and generating new MC data sets to calculate the cross section. The systematic uncertainty from this source can be ignored compared with the statistical uncertainty. The systematic uncertainty associated with the angular distribution of Σ^+ baryons is evaluated by reweighting the angular distribution of the signal MC sample to that of the data and measuring the cross section again, which is determined to be 1.3% as the difference between the reobtained cross section and the baseline value.

TABLE I. Inputs used to calculate the cross section of $\Lambda + {}^9\mathrm{Be} \to \Sigma^+ + X$.

Parameter	Value
N_{DT}	795 ± 101
ϵ_{sig}	24.32%
$\mathcal{L}_\Lambda$	$(17.00 \pm 0.01) \times 10^{28}$ cm^{-2}
$\mathcal{B}(\Sigma^+ \to p\pi^0)$	(51.57 ± 0.30)%

The double-tag efficiency has a systematic uncertainty of 0.6% arising from the fitted number of double-tagged events in the signal MC sample. The IP of the e^+e^- collision is used to calculate the track length of Λ inside the target. According to the measured result, the interaction point is distributed around the coordinate origin with an uncertainty of 0.2 cm. We change the IP within ± 0.2 cm away from the original position and take the maximum change of the measured cross section as the systematic uncertainty, which is 4.6%. The systematic uncertainty from the fit method of the $M_{p\pi^0}$ distribution is estimated by changing the background shape from a third-order Chebyshev polynomial to fourth- and fifth-order ones and assigning the uncertainty to be 3.6% as the maximum difference from the baseline result. As well as scattering inside the beam pipe and the inner wall of the MDC, the Λ hyperons may also scatter with a nucleus inside the cooling devices of the BESIII spectrometer. When calculating the luminosity $\mathcal{L}_\Lambda$, the cooling pipe is not considered due to its much more complex structure and having less material than the beam pipe and the inner wall of the MDC. We assume a conservative model of the cooling devices and measure the cross section again. The difference from the baseline result is assigned as the systematic uncertainty, which is 6.1%.

In order to estimate the systematic uncertainty caused by the assumption of the ratio of the cross sections for different kinds of nuclei, we measure the cross section again under another assumption that the cross section is proportional to the total number of protons in a nucleus. The difference from our baseline result is taken as the systematic uncertainty, which is determined to be 3.6%.

The total systematic uncertainty on the measured cross section of $\Lambda + {}^9\mathrm{Be} \to \Sigma^+ + X$ is computed to be 9.5% by adding the systematic uncertainties listed above in quadrature.

In summary, the inelastic scattering $\Lambda + {}^9\mathrm{Be} \to \Sigma^+ + X$ is studied at BESIII using a novel method. The cross section is measured to be $\sigma(\Lambda + {}^9\mathrm{Be} \to \Sigma^+ + X) = (37.3 \pm 4.7_{\mathrm{stat.}} \pm 3.5_{\mathrm{syst.}})$ mb for a Be nucleus struck by a Λ hyperon with momentum within [1.057, 1.091] GeV/c. Taking 1.93 as the ratio of the cross section of $\Lambda + {}^9\mathrm{Be} \to \Sigma^+ + X$ and $\Lambda + p \to \Sigma^+ + X$ by assuming the the signal process as a surface reaction [56–61], the cross section of $\Lambda + p \to \Sigma^+ + X$ is determined to be $\sigma(\Lambda + p \to \Sigma^+ + X) = (19.3 \pm 2.4_{\mathrm{stat.}} \pm 1.8_{\mathrm{syst.}})$ mb.

This is the first discovery and cross-section measurement of $\Lambda + p \to \Sigma^+ + n$. By virtue of charge independence, the cross sections of $\Lambda + p \to \Sigma^+ + n$ are just twice that of $\Lambda + p \to \Sigma^0 + p$ [8]. Our results are consistent with previous experiments regarding the cross-section measurement of

$\Lambda + p \to \Sigma^0 + p$ [9]. Additionally, this study represents the first attempt to investigate Λ-nucleus interactions at an e^+e^- collider. The result will be valuable for improving the understanding of the potential of strong interaction and the origin of color confinement, as well as providing important constraints for the unified model for baryon-baryon interactions. At BESIII, it is possible to measure the differential cross sections with respect to the momentum of incident hyperons using three-body decays of charmonia with at least one hyperon.

In the future, the Super τ-Charm Facility [65] will produce a J/ψ data set about 100 times larger than the sample collected by BESIII, which will allow for more detailed studies of the mechanism of hyperon-nucleon interactions.

The BESIII Collaboration thanks the staff of BEPCII and the IHEP computing center for their strong support. This work is supported in part by the National Key R&D Program of China under Contracts No. 2020YFA0406300 and No. 2020YFA0406400; the National Natural Science Foundation of China (NSFC) under Contracts No. 11635010, No. 11735014, No. 11835012, No. 11935015, No. 11935016, No. 11935018, No. 11961141012, No. 12022510, No. 12025502, No. 12035009, No. 12035013, No. 12061131003, No. 12165022, 12192260, No. 12192261, No. 12192262, No. 12192263, No. 12192264, No. 12192265, No. 12221005, No. 12225509, No. 12235017, and No. 12375071; the Chinese Academy of Sciences (CAS) Large-Scale Scientific Facility Program; the CAS Center for Excellence in Particle Physics (CCEPP); Joint Large-Scale Scientific Facility Funds of the NSFC and CAS under Contract No. U1832207; the CAS Key Research Program of Frontier Sciences under Contracts No. QYZDJ-SSW-SLH003 and No. QYZDJ-SSW-SLH040; the 100 Talents Program of CAS; the The Institute of Nuclear and Particle Physics (INPAC) and the Shanghai Key Laboratory for Particle Physics and Cosmology; the Yunnan Fundamental Research Project under Contract No. 202301AT070162; the European Union's Horizon 2020 research and innovation programme under a Marie Sklodowska-Curie grant agreement under Contract No. 894790; the German Research Foundation DFG under Contract No. 455635585, the Collaborative Research Center, CRC 1044, FOR5327, GRK 2149; the Istituto Nazionale di Fisica Nucleare, Italy; the Ministry of Development of Turkey under Contract No. DPT2006K-120470; the National Research Foundation of Korea under Contract No. NRF-2022R1A2C1092335; the National Science and Technology Fund of Mongolia; the National Science Research and Innovation Fund (NSRF) via the Program Management Unit for Human Resources & Institutional Development, Research and Innovation of Thailand under Contract No. B16F640076; the Polish National Science Centre under Contract No. 2019/35/O/ST2/02907; The Swedish Research Council; and the U. S. Department of Energy under Contract No. DE-FG02-05ER41374.

[1] I. Vidaña, Proc. R. Soc. London, Ser. A **474**, 20180145 (2018).
[2] E. Hiyama and K. Nakazawa, Annu. Rev. Nucl. Part. Sci. **68**, 131 (2018).
[3] A. Gal, E. V. Hungerford, and D. J. Millener, Rev. Mod. Phys. **88**, 035004 (2016).
[4] L. Tolos and L. Fabbietti, Prog. Part. Nucl. Phys. **112**, 103770 (2020).
[5] F. Eisele, H. Filthuth, W. Foehlisch, V. Hepp, and G. Zech, Phys. Lett. B **37**, 204 (1971).
[6] B. Sechi-Zorn, B. Kehoe, J. Twitty, and R. A. Burnstein, Phys. Rev. **175**, 1735 (1968).
[7] G. Alexander, U. Karshon, A. Shapira, G. Yekutieli, R. Engelmann, H. Filthuth, and W. Lughofer, Phys. Rev. **173**, 1452 (1968).
[8] J. A. Kadyk, G. Alexander, J. H. Chan, P. Gaposchkin, and G. H. Trilling, Nucl. Phys. B **27**, 13 (1971).
[9] J. M. Hauptman, J. A. Kadyk, and G. H. Trilling, Nucl. Phys. B **125**, 29 (1977).
[10] J. K. Ahn *et al.* (KEK-PS E-251 Collaboration), Nucl. Phys. A **648**, 263 (1999).
[11] Y. Kondo *et al.* (KEK-PS-E289 Collaboration), Nucl. Phys. A **676**, 371 (2000).
[12] J. K. Ahn, S. Aoki, K. S. Chung, M. S. Chung, H. En'yo, T. Fukuda, H. Funahashi, Y. Goto, A. Higashi, M. Ieiri *et al.* Phys. Lett. B **633**, 214 (2006).
[13] K. Miwa *et al.* (J-PARC E40 Collaboration), Phys. Rev. C **104**, 045204 (2021).
[14] K. Miwa *et al.* (J-PARC E40 Collaboration), Phys. Rev. Lett. **128**, 072501 (2022).
[15] J. Rowley *et al.* (CLAS Collaboration), Phys. Rev. Lett. **127**, 272303 (2021).
[16] T. Nanamura *et al.* (J-PARC E40 Collaboration), PTEP **2022**, 093D01 (2022).
[17] M. Ablikim *et al.* (BESIII Collaboration), Phys. Rev. Lett. **130**, 251902 (2023).
[18] S. Acharya *et al.* (ALICE Collaboration), Phys. Lett. B **844**, 137223 (2023).
[19] J. Haidenbauer and Ulf-G. Meißner, Phys. Rev. C **72**, 044005 (2005).
[20] T. A. Rijken, M. M. Nagels, and Y. Yamamoto, Prog. Theor. Phys. Suppl. **185**, 14 (2010).
[21] H. Polinder, J. Haidenbauer, and U.-G. Meißner, Nucl. Phys. A **779**, 244 (2006).
[22] J. Haidenbauer, S. Petschauer, N. Kaiser, U.-G. Meißner, A. Nogga, and W. Weise, Nucl. Phys. A **915**, 24 (2013).
[23] J. Haidenbauer, U.-G. Meißner, and S. Petschauer, Nucl. Phys. A **954**, 273 (2016).
[24] J. Haidenbauer and U.-G. Meißner, Eur. Phys. J. A **55**, 23 (2019).
[25] J. Haidenbauer, U.-G. Meißner, and A. Nogga, Eur. Phys. J. A **56**, 91 (2020).
[26] J. Haidenbauer, U.-G. Meißner, A. Nogga, and H. Le, Eur. Phys. J. A **59**, 63 (2023).
[27] K. W. Li, X. L. Ren, L. S. Geng, and B. Long, Phys. Rev. D **94**, 014029 (2016).

[28] K. W. Li, X. L. Ren, L. S. Geng, and B. W. Long, Chin. Phys. C **42**, 014105 (2018).
[29] N. Ishii, S. Aoki, and T. Hatsuda, Phys. Rev. Lett. **99**, 022001 (2007).
[30] N. Ishii *et al.* (HAL QCD Collaboration), Phys. Lett. B **712**, 437 (2012).
[31] S. R. Beane *et al.* (NPLQCD Collaboration), Nucl. Phys. A **794**, 62 (2007).
[32] S. R. Beane, W. Detmold, K. Orginos, and M. J. Savage, Prog. Part. Nucl. Phys. **66**, 1 (2011).
[33] B. J. Schaefer, M. Wagner, J. Wambach, T. T. S. Kuo, and G. E. Brown, Phys. Rev. C **73**, 011001(R) (2006).
[34] Y. Fujiwara, Y. Suzuki, and C. Nakamoto, Prog. Part. Nucl. Phys. **58**, 439 (2007).
[35] J. M. Lattimer and M. Prakash, Astrophys. J. **550**, 426 (2001).
[36] D. Lonardoni, A. Lovato, S. Gandolfi, and F. Pederiva, Phys. Rev. Lett. **114**, 092301 (2015).
[37] B. P. Abbott *et al.* (LIGO Scientific Collaboration and Virgo Collaboration), Phys. Rev. Lett. **121**, 161101 (2018).
[38] J. Dai, H.-B. Li, H. Miao, and J.-Y. Zhang, Chin. Phys. C (2024), doi:10.1088/1674-1137/ad3dde.
[39] C. Z. Yuan and M. Karliner, Phys. Rev. Lett. **127**, 012003 (2021).
[40] M. Ablikim *et al.* (BESIII Collaboration), Chin. Phys. C **46**, 074001 (2022).
[41] H. B. Li, Front. Phys. **12**, 121301 (2017); **14**, 64001 (2019).
[42] M. Ablikim *et al.* (BESIII Collaboration), Nucl. Instrum. Methods Phys. Res., Sect. A **614**, 345 (2010).
[43] See Supplemental Material at http://link.aps.org/supplemental/10.1103/PhysRevC.109.L052201 for additional information and which includes Refs. [15,56–65].
[44] S. Agostinelli *et al.* (GEANT4 Collaboration), Nucl. Instrum. Methods Phys. Res., Sect. A **506**, 250 (2003).
[45] K. X. Huang *et al.*, Nucl. Sci. Tech. **33**, 142 (2022).
[46] S. Jadach, B. F. L. Ward, and Z. Was, Nucl. Phys. B **89**, 106 (2000).
[47] D. J. Lange, Nucl. Instrum. Methods Phys. Res., Sect. A **462**, 152 (2001).
[48] R. G. Ping, Chin. Phys. C **32**, 243 (2008).
[49] R. L. Workman *et al.* (Particle Data Group), Prog. Theor. Exp. Phys. **2022**, 083C01 (2022).
[50] J. C. Chen, G. S. Huang, X. R. Qi, D. H. Zhang, and Y. S. Zhu, Phys. Rev. D **62**, 034003 (2000).
[51] R. L. Yang, R. G. Ping, and H. Chen, Chin. Phys. Lett. **31**, 061301 (2014).
[52] M. Ablikim *et al.* (BESIII Collaboration), Phys. Rev. Lett. **129**, 131801 (2022).
[53] D. H. Wright and M. H. Kelsey, Nucl. Instrum. Methods Phys. Res., Sect. A **804**, 175 (2015).
[54] R. A. Millikan, Phys. Rev. **2**, 109 (1913).
[55] NIST Chemistry webbook, https://webbook.nist.gov/chemistry/.
[56] D. S. Barton, G. W. Brandenburg, W. Busza, T. Dobrowolski, J. I. Friedman, C. Halliwell, H. W. Kendall, T. Lyons, B. Nelson, L. Rosenson *et al.*, Phys. Rev. D **27**, 2580 (1983).
[57] E. D. Cooper, B. K. Jennings, and J. Mares, Nucl. Phys. A **585**, 157 (1995).
[58] M. I. Adamovich *et al.* (WA89 Collaboration), Z. Phys. C **76**, 35 (1997).
[59] E. Botta (OBELIX Collaboration), Nucl. Phys. A **692**, 39 (2001).
[60] M. Astrua, E. Botta, T. Bressani, D. Calvo, C. Casalegno, A. Feliciello, A. Filippi, S. Marcello, M. Agnello, and F. Iazzi, Nucl. Phys. A **697**, 209 (2002).
[61] T. G. Lee and C. Y. Wong, Phys. Rev. C **97**, 054617 (2018).
[62] M. Ablikim *et al.* (BESIII Collaboration), Phys. Rev. D **104**, 072007 (2021).
[63] M. Ablikim *et al.* (BESIII Collaboration), Phys. Rev. D **81**, 052005 (2010).
[64] R. Barlow, arXiv:hep-ex/0207026.
[65] M. Achasov *et al.*, Front. Phys. **19**, 14701 (2024).

M. Ablikim,[1] M. N. Achasov,[5,b] P. Adlarson,[75] X. C. Ai,[81] R. Aliberti,[36] A. Amoroso,[74a,74c] M. R. An,[40] Q. An,[71,58] Y. Bai,[57] O. Bakina,[37] I. Balossino,[30a] Y. Ban,[47,g] V. Batozskaya,[1,45] K. Begzsuren,[33] N. Berger,[36] M. Berlowski,[45] M. Bertani,[29a] D. Bettoni,[30a] F. Bianchi,[74a,74c] E. Bianco,[74a,74c] A. Bortone,[74a,74c] I. Boyko,[37] R. A. Briere,[6] A. Brueggemann,[68] H. Cai,[76] X. Cai,[1,58] A. Calcaterra,[29a] G. F. Cao,[1,63] N. Cao,[1,63] S. A. Cetin,[62a] J. F. Chang,[1,58] T. T. Chang,[77] W. L. Chang,[1,63] G. R. Che,[44] G. Chelkov,[37,a] C. Chen,[44] Chao Chen,[55] G. Chen,[1] H. S. Chen,[1,63] M. L. Chen,[1,58,63] S. J. Chen,[43] S. L. Chen,[46] S. M. Chen,[61] T. Chen,[1,63] X. R. Chen,[32,63] X. T. Chen,[1,63] Y. B. Chen,[1,58] Y. Q. Chen,[35] Z. J. Chen,[26,h] W. S. Cheng,[74c] S. K. Choi,[11] X. Chu,[44] G. Cibinetto,[30a] S. C. Coen,[4] F. Cossio,[74c] J. J. Cui,[50] H. L. Dai,[1,58] J. P. Dai,[79] A. Dbeyssi,[19] R. E. de Boer,[4] D. Dedovich,[37] Z. Y. Deng,[1] A. Denig,[36] I. Denysenko,[37] M. Destefanis,[74a,74c] F. De Mori,[74a,74c] B. Ding,[66,1] X. X. Ding,[47,g] Y. Ding,[35] Y. Ding,[41] J. Dong,[1,58] L. Y. Dong,[1,63] M. Y. Dong,[1,58,63] X. Dong,[76] M. C. Du,[1] S. X. Du,[81] Z. H. Duan,[43] P. Egorov,[37,a] Y. H. Fan,[46] J. Fang,[1,58] S. S. Fang,[1,63] W. X. Fang,[1] Y. Fang,[1] R. Farinelli,[30a] L. Fava,[74b,74c] F. Feldbauer,[4] G. Felici,[29a] C. Q. Feng,[71,58] J. H. Feng,[59] K Fischer,[69] M. Fritsch,[4] C. D. Fu,[1] J. L. Fu,[63] Y. W. Fu,[1] H. Gao,[63] Y. N. Gao,[47,g] Yang Gao,[71,58] S. Garbolino,[74c] I. Garzia,[30a,30b] P. T. Ge,[76] Z. W. Ge,[43] C. Geng,[59] E. M. Gersabeck,[67] A Gilman,[69] K. Goetzen,[14] L. Gong,[41] W. X. Gong,[1,58] W. Gradl,[36] S. Gramigna,[30a,30b] M. Greco,[74a,74c] M. H. Gu,[1,58] Y. T. Gu,[16] C. Y Guan,[1,63] Z. L. Guan,[23] A. Q. Guo,[32,63] L. B. Guo,[42] M. J. Guo,[50] R. P. Guo,[49] Y. P. Guo,[13,f] A. Guskov,[37,a] T. T. Han,[50] W. Y. Han,[40] X. Q. Hao,[20] F. A. Harris,[65] K. K. He,[55] K. L. He,[1,63] F. H. H. Heinsius,[4] C. H. Heinz,[36] Y. K. Heng,[1,58,63] C. Herold,[60] T. Holtmann,[4] P. C. Hong,[13,f] G. Y. Hou,[1,63] X. T. Hou,[1,63] Y. R. Hou,[63] Z. L. Hou,[1] H. M. Hu,[1,63] J. F. Hu,[56,i] T. Hu,[1,58,63] Y. Hu,[1] G. S. Huang,[71,58] K. X. Huang,[59] L. Q. Huang,[32,63] X. T. Huang,[50] Y. P. Huang,[1] T. Hussain,[73] N Hüsken,[28,36] N. in der Wiesche,[68] M. Irshad,[71,58] J. Jackson,[28] S. Jaeger,[4] S. Janchiv,[33] J. H. Jeong,[11] Q. Ji,[1] Q. P. Ji,[20] X. B. Ji,[1,63] X. L. Ji,[1,58] Y. Y. Ji,[50] X. Q. Jia,[50] Z. K. Jia,[71,58] H. J. Jiang,[76] P. C. Jiang,[47,g] S. S. Jiang,[40] T. J. Jiang,[17] X. S. Jiang,[1,58,63] Y. Jiang,[63] J. B. Jiao,[50] Z. Jiao,[24] S. Jin,[43] Y. Jin,[66] M. Q. Jing,[1,63] T. Johansson,[75] X. K.,[1] S. Kabana,[34]

N. Kalantar-Nayestanaki,[64] X. L. Kang,[10] X. S. Kang,[41] M. Kavatsyuk,[64] B. C. Ke,[81] A. Khoukaz,[68] R. Kiuchi,[1] R. Kliemt,[14] O. B. Kolcu,[62a] B. Kopf,[4] M. Kuessner,[4] A. Kupsc,[45,75] W. Kühn,[38] J. J. Lane,[67] P. Larin,[19] A. Lavania,[27] L. Lavezzi,[74a,74c] T. T. Lei,[71,58] Z. H. Lei,[71,58] H. Leithoff,[36] M. Lellmann,[36] T. Lenz,[36] C. Li,[44] C. Li,[48] C. H. Li,[40] Cheng Li,[71,58] D. M. Li,[81] F. Li,[1,58] G. Li,[1] H. Li,[71,58] H. B. Li,[1,63] H. J. Li,[20] H. N. Li,[56,i] Hui Li,[44] J. R. Li,[61] J. S. Li,[59] J. W. Li,[50] K. L. Li,[20] Ke Li,[1] L. J Li,[1,63] L. K. Li,[1] Lei Li,[3] M. H. Li,[44] P. R. Li,[39,j,k] Q. X. Li,[50] S. X. Li,[13] T. Li,[50] W. D. Li,[1,63] W. G. Li,[1] X. H. Li,[71,58] X. L. Li,[50] Xiaoyu Li,[1,63] Y. G. Li,[47,g] Z. J. Li,[59] Z. X. Li,[16] C. Liang,[43] H. Liang,[1,63] H. Liang,[35] H. Liang,[71,58] Y. F. Liang,[54] Y. T. Liang,[32,63] G. R. Liao,[15] L. Z. Liao,[50] Y. P. Liao,[1,63] J. Libby,[27] A. Limphirat,[60] D. X. Lin,[32,63] T. Lin,[1] B. J. Liu,[1] B. X. Liu,[76] C. Liu,[35] C. X. Liu,[1] F. H. Liu,[53] Fang Liu,[1] Feng Liu,[7] G. M. Liu,[56,i] H. Liu,[39,j,k] H. B. Liu,[16] H. M. Liu,[1,63] Huanhuan Liu,[1] Huihui Liu,[22] J. B. Liu,[71,58] J. L. Liu,[72] J. Y. Liu,[1,63] K. Liu,[1] K. Y. Liu,[41] Ke Liu,[23] L. Liu,[71,58] L. C. Liu,[44] Lu Liu,[44] M. H. Liu,[13,f] P. L. Liu,[1] Q. Liu,[63] S. B. Liu,[71,58] T. Liu,[13,f] W. K. Liu,[44] W. M. Liu,[71,58] X. Liu,[39,j,k] Y. Liu,[39,j,k] Y. Liu,[81] Y. B. Liu,[44] Z. A. Liu,[1,58,63] Z. Q. Liu,[50] X. C. Lou,[1,58,63] F. X. Lu,[59] H. J. Lu,[24] J. G. Lu,[1,58] X. L. Lu,[1] Y. Lu,[8] Y. P. Lu,[1,58] Z. H. Lu,[1,63] C. L. Luo,[42] M. X. Luo,[80] T. Luo,[13,f] X. L. Luo,[1,58] X. R. Lyu,[63] Y. F. Lyu,[44] F. C. Ma,[41] H. L. Ma,[1] J. L. Ma,[1,63] L. L. Ma,[50] M. M. Ma,[1,63] Q. M. Ma,[1] R. Q. Ma,[1,63] R. T. Ma,[63] X. Y. Ma,[1,58] Y. Ma,[47,g] Y. M. Ma,[32] F. E. Maas,[19] M. Maggiora,[74a,74c] S. Malde,[69] Q. A. Malik,[73] A. Mangoni,[29b] Y. J. Mao,[47,g] Z. P. Mao,[1] S. Marcello,[74a,74c] Z. X. Meng,[66] J. G. Messchendorp,[14,64] G. Mezzadri,[30a] H. Miao,[1,63] T. J. Min,[43] R. E. Mitchell,[28] X. H. Mo,[1,58,63] N. Yu. Muchnoi,[5,b] J. Muskalla,[36] Y. Nefedov,[37] F. Nerling,[19,d] I. B. Nikolaev,[5,b] Z. Ning,[1,58] S. Nisar,[12,l] Q. L. Niu,[39,j,k] W. D. Niu,[55] Y. Niu,[50] S. L. Olsen,[63] Q. Ouyang,[1,58,63] S. Pacetti,[29b,29c] X. Pan,[55] Y. Pan,[57] A. Pathak,[35] P. Patteri,[29a] Y. P. Pei,[71,58] M. Pelizaeus,[4] H. P. Peng,[71,58] Y. Y. Peng,[39,j,k] K. Peters,[14,d] J. L. Ping,[42] R. G. Ping,[1,63] S. Plura,[36] V. Prasad,[34] F. Z. Qi,[1] H. Qi,[71,58] H. R. Qi,[61] M. Qi,[43] T. Y. Qi,[13,f] S. Qian,[1,58] W. B. Qian,[63] C. F. Qiao,[63] J. J. Qin,[72] L. Q. Qin,[15] X. P. Qin,[13,f] X. S. Qin,[50] Z. H. Qin,[1,58] J. F. Qiu,[1] S. Q. Qu,[61] C. F. Redmer,[36] K. J. Ren,[40] A. Rivetti,[74c] M. Rolo,[74c] G. Rong,[1,63] Ch. Rosner,[19] S. N. Ruan,[44] N. Salone,[45] A. Sarantsev,[37,c] Y. Schelhaas,[36] K. Schoenning,[75] M. Scodeggio,[30a,30b] K. Y. Shan,[13,f] W. Shan,[25] X. Y. Shan,[71,58] J. F. Shangguan,[55] L. G. Shao,[1,63] M. Shao,[71,58] C. P. Shen,[13,f] H. F. Shen,[1,63] W. H. Shen,[63] X. Y. Shen,[1,63] B. A. Shi,[63] H. C. Shi,[71,58] J. L. Shi,[13] J. Y. Shi,[1] Q. Q. Shi,[55] R. S. Shi,[1,63] X. Shi,[1,58] J. J. Song,[20] T. Z. Song,[59] W. M. Song,[35,1] Y. J. Song,[13] Y. X. Song,[47,g] S. Sosio,[74a,74c] S. Spataro,[74a,74c] F. Stieler,[36] Y. J. Su,[63] G. B. Sun,[76] G. X. Sun,[1] H. Sun,[63] H. K. Sun,[1] J. F. Sun,[20] K. Sun,[61] L. Sun,[76] S. S. Sun,[1,63] T. Sun,[1,63] W. Y. Sun,[35] Y. Sun,[10] Y. J. Sun,[71,58] Y. Z. Sun,[1] Z. T. Sun,[50] Y. X. Tan,[71,58] C. J. Tang,[54] G. Y. Tang,[1] J. Tang,[59] Y. A. Tang,[76] L. Y. Tao,[72] Q. T. Tao,[26,h] M. Tat,[69] J. X. Teng,[71,58] V. Thoren,[75] W. H. Tian,[59] W. H. Tian,[52] Y. Tian,[32,63] Z. F. Tian,[76] I. Uman,[62b] S. J. Wang,[50] B. Wang,[1] B. L. Wang,[63] Bo Wang,[71,58] C. W. Wang,[43] D. Y. Wang,[47,g] F. Wang,[72] H. J. Wang,[39,j,k] H. P. Wang,[1,63] J. P. Wang,[50] K. Wang,[1,58] L. L. Wang,[1] M. Wang,[50] Meng Wang,[1,63] S. Wang,[13,f] S. Wang,[39,j,k] T. Wang,[13,f] T. J. Wang,[44] W. Wang,[72] W. Wang,[59] W. P. Wang,[71,58] X. Wang,[47,g] X. F. Wang,[39,j,k] X. J. Wang,[40] X. L. Wang,[13,f] Y. Wang,[61] Y. D. Wang,[46] Y. F. Wang,[1,58,63] Y. H. Wang,[48] Y. N. Wang,[46] Y. Q. Wang,[1] Yaqian Wang,[18,1] Yi Wang,[61] Z. Wang,[1,58] Z. L. Wang,[72] Z. Y. Wang,[1,63] Ziyi Wang,[63] D. Wei,[70] D. H. Wei,[15] F. Weidner,[68] S. P. Wen,[1] C. W. Wenzel,[4] U. Wiedner,[4] G. Wilkinson,[69] M. Wolke,[75] L. Wollenberg,[4] C. Wu,[40] J. F. Wu,[1,63] L. H. Wu,[1] L. J. Wu,[1,63] X. Wu,[13,f] X. H. Wu,[35] Y. Wu,[71] Y. H. Wu,[55] Y. J. Wu,[32] Z. Wu,[1,58] L. Xia,[71,58] X. M. Xian,[40] T. Xiang,[47,g] D. Xiao,[39,j,k] G. Y. Xiao,[43] S. Y. Xiao,[1] Y. L. Xiao,[13,f] Z. J. Xiao,[42] C. Xie,[43] X. H. Xie,[47,g] Y. Xie,[50] Y. G. Xie,[1,58] Y. H. Xie,[7] Z. P. Xie,[71,58] T. Y. Xing,[1,63] C. F. Xu,[1,63] C. J. Xu,[59] G. F. Xu,[1] H. Y. Xu,[66] Q. J. Xu,[17] Q. N. Xu,[31] W. Xu,[1,63] W. L. Xu,[66] X. P. Xu,[55] Y. C. Xu,[78] Z. P. Xu,[43] Z. S. Xu,[63] F. Yan,[13,f] L. Yan,[13,f] W. B. Yan,[71,58] W. C. Yan,[81] X. Q. Yan,[1] H. J. Yang,[51,e] H. L. Yang,[35] H. X. Yang,[1] Tao Yang,[1] Y. Yang,[13,f] Y. F. Yang,[44] Y. X. Yang,[1,63] Yifan Yang,[1,63] Z. W. Yang,[39,j,k] Z. P. Yao,[50] M. Ye,[1,58] M. H. Ye,[9] J. H. Yin,[1] Z. Y. You,[59] B. X. Yu,[1,58,63] C. X. Yu,[44] G. Yu,[1,63] J. S. Yu,[26,h] T. Yu,[72] X. D. Yu,[47,g] C. Z. Yuan,[1,63] L. Yuan,[2] S. C. Yuan,[1] X. Q. Yuan,[1] Y. Yuan,[1,63] Z. Y. Yuan,[59] C. X. Yue,[40] A. A. Zafar,[73] F. R. Zeng,[50] X. Zeng,[13,f] Y. Zeng,[26,h] Y. J. Zeng,[1,63] X. Y. Zhai,[35] Y. C. Zhai,[50] Y. H. Zhan,[59] A. Q. Zhang,[1,63] B. L. Zhang,[1,63] B. X. Zhang,[1] D. H. Zhang,[44] G. Y. Zhang,[20] H. Zhang,[71] H. C. Zhang,[1,58,63] H. H. Zhang,[59] H. H. Zhang,[35] H. Q. Zhang,[1,58,63] H. Y. Zhang,[1,58] J. Zhang,[81] J. J. Zhang,[52] J. L. Zhang,[21] J. Q. Zhang,[42] J. W. Zhang,[1,58,63] J. X. Zhang,[39,j,k] J. Y. Zhang,[1] J. Z. Zhang,[1,63] Jianyu Zhang,[63] Jiawei Zhang,[1,63] L. M. Zhang,[61] L. Q. Zhang,[59] Lei Zhang,[43] P. Zhang,[1,63] Q. Y. Zhang,[40,81] Shuihan Zhang,[1,63] Shulei Zhang,[26,h] X. D. Zhang,[46] X. M. Zhang,[1] X. Y. Zhang,[50] Xuyan Zhang,[55] Y. Zhang,[69] Y. Zhang,[72] Y. T. Zhang,[81] Y. H. Zhang,[1,58] Yan Zhang,[71,58] Yao Zhang,[1] Z. H. Zhang,[1] Z. L. Zhang,[35] Z. Y. Zhang,[44] Z. Y. Zhang,[76] G. Zhao,[1] J. Zhao,[40] J. Y. Zhao,[1,63] J. Z. Zhao,[1,58] Lei Zhao,[71,58] Ling Zhao,[1] M. G. Zhao,[44] S. J. Zhao,[81] Y. B. Zhao,[1,58] Y. X. Zhao,[32,63] Z. G. Zhao,[71,58] A. Zhemchugov,[37,a] B. Zheng,[72] J. P. Zheng,[1,58] W. J. Zheng,[1,63] Y. H. Zheng,[63] B. Zhong,[42] X. Zhong,[59] H. Zhou,[50] L. P. Zhou,[1,63] X. Zhou,[76] X. K. Zhou,[7] X. R. Zhou,[71,58] X. Y. Zhou,[40] Y. Z. Zhou,[13,f] J. Zhu,[44] K. Zhu,[1] K. J. Zhu,[1,58,63] L. Zhu,[35] L. X. Zhu,[63] S. H. Zhu,[70] S. Q. Zhu,[43] T. J. Zhu,[13,f] W. J. Zhu,[13,f] Y. C. Zhu,[71,58] Z. A. Zhu,[1,63] J. H. Zou,[1] and J. Zu[71,58]

(BESIII Collaboration)

[1]*Institute of High Energy Physics, Beijing 100049, People's Republic of China*
[2]*Beihang University, Beijing 100191, People's Republic of China*
[3]*Beijing Institute of Petrochemical Technology, Beijing 102617, People's Republic of China*
[4]*Bochum Ruhr-University, D-44780 Bochum, Germany*

[5]*Budker Institute of Nuclear Physics SB RAS (BINP), Novosibirsk 630090, Russia*
[6]*Carnegie Mellon University, Pittsburgh, Pennsylvania 15213, USA*
[7]*Central China Normal University, Wuhan 430079, People's Republic of China*
[8]*Central South University, Changsha 410083, People's Republic of China*
[9]*China Center of Advanced Science and Technology, Beijing 100190, People's Republic of China*
[10]*China University of Geosciences, Wuhan 430074, People's Republic of China*
[11]*Chung-Ang University, Seoul 06974, Republic of Korea*
[12]*COMSATS University Islamabad, Lahore Campus, Defence Road, Off Raiwind Road, 54000 Lahore, Pakistan*
[13]*Fudan University, Shanghai 200433, People's Republic of China*
[14]*GSI Helmholtzcentre for Heavy Ion Research GmbH, D-64291 Darmstadt, Germany*
[15]*Guangxi Normal University, Guilin 541004, People's Republic of China*
[16]*Guangxi University, Nanning 530004, People's Republic of China*
[17]*Hangzhou Normal University, Hangzhou 310036, People's Republic of China*
[18]*Hebei University, Baoding 071002, People's Republic of China*
[19]*Helmholtz Institute Mainz, Staudinger Weg 18, D-55099 Mainz, Germany*
[20]*Henan Normal University, Xinxiang 453007, People's Republic of China*
[21]*Henan University, Kaifeng 475004, People's Republic of China*
[22]*Henan University of Science and Technology, Luoyang 471003, People's Republic of China*
[23]*Henan University of Technology, Zhengzhou 450001, People's Republic of China*
[24]*Huangshan College, Huangshan 245000, People's Republic of China*
[25]*Hunan Normal University, Changsha 410081, People's Republic of China*
[26]*Hunan University, Changsha 410082, People's Republic of China*
[27]*Indian Institute of Technology Madras, Chennai 600036, India*
[28]*Indiana University, Bloomington, Indiana 47405, USA*
[29a]*INFN Laboratori Nazionali di Frascati, INFN Laboratori Nazionali di Frascati, I-00044 Frascati, Italy*
[29b]*INFN Laboratori Nazionali di Frascati, INFN Sezione di Perugia, I-06100 Perugia, Italy*
[29c]*INFN Laboratori Nazionali di Frascati, University of Perugia, I-06100 Perugia, Italy*
[30a]*INFN Sezione di Ferrara, INFN Sezione di Ferrara, I-44122 Ferrara, Italy*
[30b]*INFN Sezione di Ferrara, University of Ferrara, I-44122 Ferrara, Italy*
[31]*Inner Mongolia University, Hohhot 010021, People's Republic of China*
[32]*Institute of Modern Physics, Lanzhou 730000, People's Republic of China*
[33]*Institute of Physics and Technology, Peace Avenue 54B, Ulaanbaatar 13330, Mongolia*
[34]*Instituto de Alta Investigación, Universidad de Tarapacá, Casilla 7D, Arica 1000000, Chile*
[35]*Jilin University, Changchun 130012, People's Republic of China*
[36]*Johannes Gutenberg University of Mainz, Johann-Joachim-Becher-Weg 45, D-55099 Mainz, Germany*
[37]*Joint Institute for Nuclear Research, 141980 Dubna, Moscow Region, Russia*
[38]*Justus-Liebig-Universitaet Giessen, II. Physikalisches Institut, Heinrich-Buff-Ring 16, D-35392 Giessen, Germany*
[39]*Lanzhou University, Lanzhou 730000, People's Republic of China*
[40]*Liaoning Normal University, Dalian 116029, People's Republic of China*
[41]*Liaoning University, Shenyang 110036, People's Republic of China*
[42]*Nanjing Normal University, Nanjing 210023, People's Republic of China*
[43]*Nanjing University, Nanjing 210093, People's Republic of China*
[44]*Nankai University, Tianjin 300071, People's Republic of China*
[45]*National Centre for Nuclear Research, Warsaw 02-093, Poland*
[46]*North China Electric Power University, Beijing 102206, People's Republic of China*
[47]*Peking University, Beijing 100871, People's Republic of China*
[48]*Qufu Normal University, Qufu 273165, People's Republic of China*
[49]*Shandong Normal University, Jinan 250014, People's Republic of China*
[50]*Shandong University, Jinan 250100, People's Republic of China*
[51]*Shanghai Jiao Tong University, Shanghai 200240, People's Republic of China*
[52]*Shanxi Normal University, Linfen 041004, People's Republic of China*
[53]*Shanxi University, Taiyuan 030006, People's Republic of China*
[54]*Sichuan University, Chengdu 610064, People's Republic of China*
[55]*Soochow University, Suzhou 215006, People's Republic of China*
[56]*South China Normal University, Guangzhou 510006, People's Republic of China*
[57]*Southeast University, Nanjing 211100, People's Republic of China*
[58]*State Key Laboratory of Particle Detection and Electronics, Beijing 100049, Hefei 230026, People's Republic of China*
[59]*Sun Yat-Sen University, Guangzhou 510275, People's Republic of China*
[60]*Suranaree University of Technology, University Avenue 111, Nakhon Ratchasima 30000, Thailand*

[61] *Tsinghua University, Beijing 100084, People's Republic of China*
[62a] *Turkish Accelerator Center Particle Factory Group, Istinye University, 34010 Istanbul, Turkey*
[62b] *Turkish Accelerator Center Particle Factory Group, Near East University, Nicosia, North Cyprus, 99138 Mersin 10, Turkey*
[63] *University of Chinese Academy of Sciences, Beijing 100049, People's Republic of China*
[64] *University of Groningen, NL-9747 AA Groningen, The Netherlands*
[65] *University of Hawaii, Honolulu, Hawaii 96822, USA*
[66] *University of Jinan, Jinan 250022, People's Republic of China*
[67] *University of Manchester, Oxford Road, Manchester M13 9PL, United Kingdom*
[68] *University of Muenster, Wilhelm-Klemm-Strasse 9, 48149 Muenster, Germany*
[69] *University of Oxford, Keble Road, Oxford OX13RH, United Kingdom*
[70] *University of Science and Technology Liaoning, Anshan 114051, People's Republic of China*
[71] *University of Science and Technology of China, Hefei 230026, People's Republic of China*
[72] *University of South China, Hengyang 421001, People's Republic of China*
[73] *University of the Punjab, Lahore 54590, Pakistan*
[74a] *University of Turin and INFN, University of Turin, I-10125 Turin, Italy*
[74b] *University of Turin and INFN, University of Eastern Piedmont, I-15121 Alessandria, Italy*
[74c] *University of Turin and INFN, INFN, I-10125 Turin, Italy*
[75] *Uppsala University, Box 516, SE-75120 Uppsala, Sweden*
[76] *Wuhan University, Wuhan 430072, People's Republic of China*
[77] *Xinyang Normal University, Xinyang 464000, People's Republic of China*
[78] *Yantai University, Yantai 264005, People's Republic of China*
[79] *Yunnan University, Kunming 650500, People's Republic of China*
[80] *Zhejiang University, Hangzhou 310027, People's Republic of China*
[81] *Zhengzhou University, Zhengzhou 450001, People's Republic of China*

[a] Also at the Moscow Institute of Physics and Technology, Moscow 141700, Russia.
[b] Also at the Novosibirsk State University, Novosibirsk, 630090, Russia.
[c] Also at the NRC "Kurchatov Institute", PNPI, 188300 Gatchina, Russia.
[d] Also at Goethe University Frankfurt, 60323 Frankfurt am Main, Germany.
[e] Also at Key Laboratory for Particle Physics, Astrophysics and Cosmology, Ministry of Education; Shanghai Key Laboratory for Particle Physics and Cosmology; Institute of Nuclear and Particle Physics, Shanghai 200240, People's Republic of China.
[f] Also at Key Laboratory of Nuclear Physics and Ion-beam Application (MOE) and Institute of Modern Physics, Fudan University, Shanghai 200443, People's Republic of China.
[g] Also at State Key Laboratory of Nuclear Physics and Technology, Peking University, Beijing 100871, People's Republic of China.
[h] Also at School of Physics and Electronics, Hunan University, Changsha 410082, China.
[i] Also at Guangdong Provincial Key Laboratory of Nuclear Science, Institute of Quantum Matter, South China Normal University, Guangzhou 510006, China.
[j] Also at Frontiers Science Center for Rare Isotopes, Lanzhou University, Lanzhou 730000, People's Republic of China.
[k] Also at Lanzhou Center for Theoretical Physics, Lanzhou University, Lanzhou 730000, People's Republic of China.
[l] Also at the Department of Mathematical Sciences, IBA, Karachi 75270, Pakistan.